Solubility and Charge Transport in Blends of Poly-dialkoxy-p-phenylene Vinylene and UV-Cross-Linkable Matrices

Kasparek, C.; Rohloff, R.; Michels, J. J.; Craciun, N. I.; Wildeman, J.; Blom, P. W. M.

Published in:
Advanced electronic materials

DOI:
10.1002/aelm.201600519

ADVANCED ELECTRONIC MATERIALS
www.advelectronicmat.de

Solubility and Charge Transport in Blends of Poly-dialkoxy-*p*-phenylene Vinylene and UV-Cross-Linkable Matrices

*C. Kasparek, R. Rohloff, J. J. Michels, N. I. Crăciun, J. Wildeman, and P. W. M. Blom**

Poly[2-methoxy-5-(2-ethylhexyloxy)-1,4-phenylenevinylene] (MEH-PPV) is blended with two different inert UV-cross-linkable matrices to tune the solubility of the solution-processed films. It is found that only 10 wt% of theses matrices is required to make the blend layer insoluble after cross-linking. The addition of only 10 wt% matrix only slightly reduces the hole mobility, whereas the electron transport is not affected. Polymer light-emitting diodes (PLEDs) with an insoluble 90:10 MEH-PPV: matrix blend layer exhibit the same current density and photocurrent as pristine MEH-PPV PLEDs.

1. Introduction

Organic light-emitting diodes (OLEDs) consist of a stack of small molecule-based layers that each has specific functions.[1] These functions include hole transport, electron blocking, emission of one or more colors, hole blocking, and electron transport. Conventionally, such a stack of layers is deposited by thermal evaporation in a high vacuum. The route toward lower cost is to process these layers from solution, such that a cost efficient roll-to-roll process can be used. However, a major challenge is the stack integrity; when a subsequent layer is coated on top of a previously deposited layer, the first layer will redissolve in the solvent of the second layer.

In the last years a lot of effort has been done to overcome this problem. A common approach is to use orthogonal solvents for two adjacent layers.[2–9] By alternating polar and nonpolar solvents for the layers, the following deposition will not dissolve the first layer. A different technique is to add cross-linkable side chains to the functional material. These are then cross-linked using ultraviolet (UV) light. This prevents redissolution during the deposition of a subsequent layer.[10–15] Additionally to UV-cross-linking, thermal cross-linking of pristine films of a hole transport layer has been successfully shown.[16–18] Recently, Aizawa et al. combined thermally cross-linkable materials and orthogonal solvents to achieve a high-efficiency solution-processed white-light emitting small molecule OLED.[10] A different approach using cross-linking was shown by Png et al. by adding fluorophenyl azides that cross-link the alkyl side chains of commercially available polymers, resulting in an insoluble layer.[19]

Another proposed option is the use of a liquid buffer layer. Here, a buffer layer is deposited on top of the first layer. The buffer layer does not dissolve in the solvents of the subsequent layer. The second layer then floats on top of the buffer layer. The buffer layer evaporates either during the deposition or during a subsequent baking step.[20,21] Furthermore, it has been shown that for polymers also differences in molecular weight can be used to realize a bilayer structure. Polymers with a high molecular weight take a long time to dissolve in solvents such that a second layer can be processed on top.[22] Recently, He et al. reported that cross-linking the surface using a mixed acetylene and argon plasma makes it possible to resist redissolution in organic solvents.[23] An excellent review of the recent progress of solution-processed multilayer OLEDs is given by So and co-workers.[24]

These approaches all have certain disadvantages, for example, multilayer structures based on solvent polarity or cross-linkable units typically rely on elaborate and often cumbersome synthetic strategies. The approaches involving liquid buffer layers or molecular weight differences only allow for a limited number of layers in the final stack. An interesting alternative approach has been published by Zhou et al.[25] A polyfluorene-based hole transport material was blended with two insulating, commercially available cross-linkable materials, ethoxylated (4) bisphenol a dimethacrylate (SR540, Sartomer), and NOA83H (Norland Products), to tune the solubility of the resulting blend layer. Upon cross-linking with UV-light these materials form an insoluble host matrix around the semiconductor that makes the whole blend layer insoluble.

In contrast to the approaches mentioned before, in this approach standard organic semiconductors can be used without the requirement for chemical modifications. However, in order to make the layer insoluble in either toluene and chloroform these blends contained nearly 70% of cross-linkable host matrix, which might have a severe effect on the charge transport properties. Nevertheless, an improved performance of a polymer light-emitting diode (PLED) containing such an insoluble hole transport layer was observed. To further validate this approach knowledge on the effect of the amount of matrix on the solubility and the charge transport properties of the

C. Kasparek, R. Rohloff, Dr. J. J. Michels, Dr. N. I. Crăciun,
Prof. P. W. M. Blom
Max Planck Institute for Polymer Research
Ackermannweg 10, 55128 Mainz, Germany
E-mail: blom@mpip-mainz.mpg.de
C. Kasparek
Dutch Polymer Institute
P.O. Box 902, 5600 AX, Eindhoven, The Netherlands
J. Wildeman
Zernike Institute for Advanced Materials
University of Groningen
Nijenborgh 4, 9747 AG, Groningen, The Netherlands

DOI: 10.1002/aelm.201600519

semiconducting polyfluorene derivative is a prerequisite but was not systematically investigated.

In this work, we extend the approach of Zhou et al. using the model material poly[2-methoxy-5-(2-ethylhexyloxy)-1,4-phenylenevinylene] (MEH-PPV) as an emitting polymer layer. We use the same commercial UV-cross-linkable inert host matrices NOA83H and SR540 in a blend with MEH-PPV. In contrast to the work of Zhou et al., we find that only a small amount of 10 wt% of the insulating matrix is needed to make the blend layer insoluble for chlorobenzene. Additionally, we analyzed the hole and electron transport of the blend layers. For only 10% matrix the charge transport properties were barely affected. From the insoluble blend layers PLEDs could be fabricated with identical current and efficiency as pristine MEH-PPV devices.

2. Results and Discussion

2.1. Tuning the Solubility of a MEH-PPV: Matrix Blend Layer

Blends of MEH-PPV and SR540 in different concentrations, ranging from 20:80 MEH-PPV: SR540 to pristine MEH-PPV (100%), were made and spin coated on a glass substrate. The notation 20:80 MEH-PPV: SR540 means that there is 20 wt% MEH-PPV and 80 wt% SR540 in the blend. The blends were cross-linked with a dose of 3 J cm^{-2} in a nitrogen atmosphere. The film thickness of all blends was around 100 nm after cross-linking.[26] To test the effectiveness of the cross-linking procedure, chlorobenzene was spin coated on top of the cured blend films to remove any dissolvable material, followed by measurement of the film thickness. Since MEH-PPV is well soluble in chlorobenzene, parts of the MEH-PPV in the blend that are not surrounded by matrix can be washed off. The difference in film thickness ΔL before and after spin-coating chlorobenzene on top is plotted as a function of the concentration of MEH-PPV in **Figure 1**a). From the 100 nm of the pristine MEH-PPV film around 60 nm was washed off. The wash-off is not complete due to the relatively high molecular weight (M_w = 350 000 g mol^{-1}) of the MEH-PPV used. Adding only 5% of the SR540 matrix decreased the wash-off to 20 nm after cross-linking. The wash-off for a blend containing 10% SR540 was around 15 nm. Further increasing the amount of SR540 to 20% decreased the wash-off to 10 nm. The blends from 80:20 down to 20:80 MEH-PPV: SR540 showed a wash-off of less than 10 nm. We note that such small wash-off approaches the accuracy of the profilometric thickness measurement, which is typically 5 nm. Surprisingly, only small concentrations of 10%–20% SR540 in the blend are sufficient to drastically reduce the solubility of the film. In this case MEH-PPV is in excess of SR540; however, the term matrix for SR540 and NOA83H will be further used.

To investigate the influence of the UV-illumination dose, blends of 90:10 MEH-PPV: SR540 and 90:10 MEH-PPV: NOA83H were cross-linked with different doses. Again, the film thickness of the cross-linked samples was measured before and after spin-coating chlorobenzene on top. The resulting difference in film thickness ΔL is plotted against the UV dose in Figure 1b. For both matrices (SR540 in black and NOA83H in red) the thickness difference of the blend decreases with increasing dose. For a sufficiently high dose of typically 40 J cm^{-2}, the wash-off for the 90:10 MEH-PPV: matrix blend can even be decreased close to 0 nm, resulting in completely insoluble films.

To show that the solubility is low enough to allow for sequential solution processing, four layers of a 90:10 MEH-PPV: SR540 blend were stacked on top of each other. To this end, first a single layer was spin coated and cross-linked with a dose of 43 J cm^{-2} and the film thickness was measured. Afterward, a subsequent layer was spin coated on top of the first one and the total thickness was measured again after cross-linking. This was repeated for four layers in total. The total film thickness is plotted against the number of layers in Figure 1c. As expected for an insoluble film, the film thickness increases linearly with the number of deposited layers. The red line shows a linear fit with a slope of 70 nm per layer. This is in good agreement with the measured thickness of the first layer of 75 nm.[27] As a result, for both matrices we demonstrated that with a sufficiently large UV-illumination dose the 90:10 MEH-PPV: matrix blends are completely insoluble.

2.2. Hole Transport in the MEH-PPV: Matrix Blends

2.2.1. MEH-PPV: NOA83H Blends

As a next step we investigate how the presence of the electrically inert matrix affects the transport of holes through the MEH-PPV: matrix blend. **Figure 2**a shows the *J*–*V* characteristics at

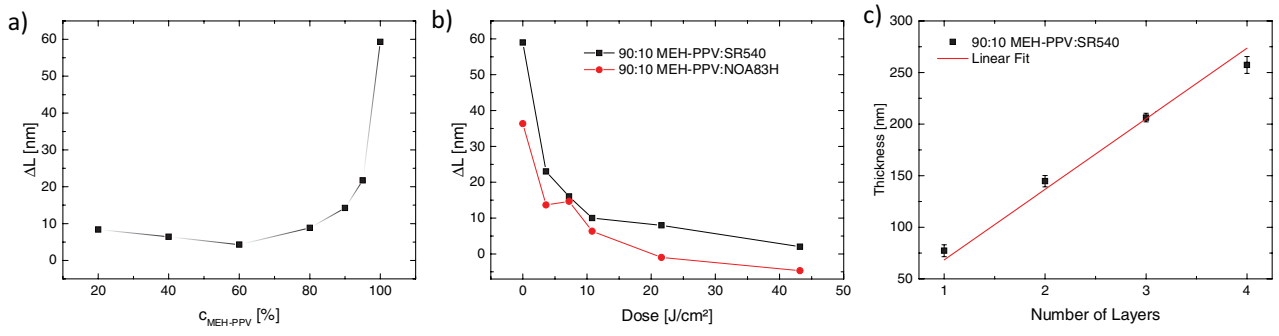

Figure 1. a) Film thickness difference after spin-coating chlorobenzene on top of the cross-linked MEH-PPV: SR540 blends (dose 3 J cm^{-2}) for different ratios of MEH-PPV and SR540. b) Film thickness difference of MEH-PPV blended with SR540 (black) and NOA83H (red) in a 90:10 ratio for different doses. c) Film thickness of 90:10 MEH-PPV: SR540 layers that were each cross-linked with a dose of 43 J cm^{-2} stacked on top of each other.

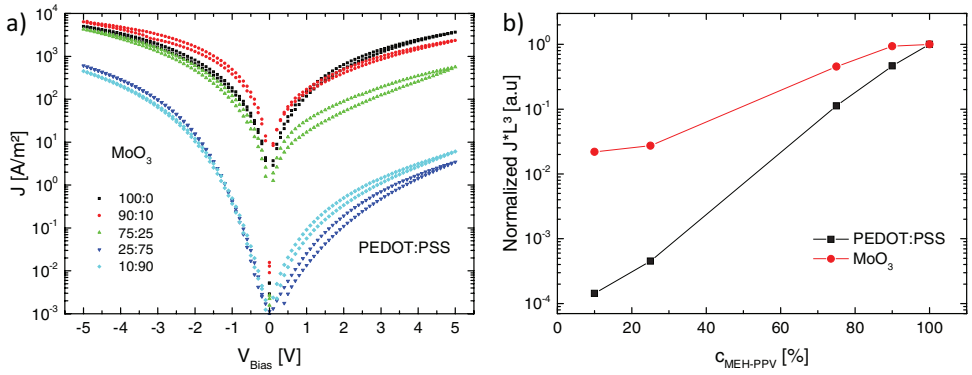

Figure 2. a) Current density–voltage characteristics at room temperature of MEH-PPV: NOA83H hole only devices. Forward bias shows injection from PEDOT: PSS, reverse bias shows injection from MoO_3. b) Current density at +2 V (injection from PEDOT: PSS, black) and −2 V (injection from MoO_3, red) corrected for the film thickness. The blends were cross-linked with a dose of 43 J cm^{-1}.

room temperature of hole-only devices of MEH-PPV: NOA83H blends from pristine MEH-PPV (100:0) all the way down to 10:90 blends with only 10% of the conducting MEH-PPV. The device structure of the hole-only devices is ITO/poly(3,4-ethylenedioxythiophene) polystyrene sulfonate (PEDOT: PSS)/MEH-PPV: NOA83H/MoO_3/Al (see the Experimental Section). The blends were cross-linked with a dose of 43 J cm^{-1}. The *J*–*V* curve of the pristine MEH-PPV hole-only device (black squares) is symmetric in forward- and reverse bias. This is in agreement with the observation that PEDOT: PSS and MoO_3 both form an Ohmic contact to the HOMO of MEH-PPV.[28] However, if there is only 10% of NOA83H in the blend, the curve becomes asymmetric. When the holes are injected from the MoO_3 top contact (reverse bias), the current density is higher as compared to hole injection from the PEDOT: PSS bottom contact (forward bias). The asymmetry is small for the 90:10 MEH-PPV: NOA83H device, but for blends with a higher concentration of NOA83H the asymmetry steadily grows. For the 10:90 MEH-PPV: NOA83H blend a difference of more than two orders of magnitude between forward- and reverse bias is observed.

To visualize the effect of the NOA38H on the magnitude of the hole current in Figure 2b, current density at +2 and −2 V is plotted as a function of the concentration of MEH-PPV in the blend. For pristine MEH-PPV the (symmetric) current is known to be space-charge limited, following the Mott–Gurney law $J = \frac{9}{8}\varepsilon_0\varepsilon_r\mu\frac{V^2}{L^3}$ at low voltages.[29] Not all film thicknesses are identical for the different blend ratios. Therefore, we correct for the effect of thickness variation by multiplying the measured current density *J* at +2 V and −2 V with the film thickness *L* to the third power, according to the Mott–Gurney law. As mentioned above, the current density at +2 V shows the current when holes are injected from the PEDOT: PSS contact, whereas the current density at −2 V shows the hole current injected from the MoO_3 contact. For hole injection from the PEDOT: PSS contact the current density strongly decreases with decreasing amount of MEH-PPV in the blend. The difference in current density between 100% MEH-PPV and 10:90 MEH-PPV: NOA83H amounts to four orders of magnitude. In contrast, the current density for hole injection from the MoO_3 contact hardly changes for concentrations of 100% MEH-PPV down to 75:25 MEH-PPV: NOA83H. Only if the concentration of MEH-PPV is further reduced to 25% the current density decreases by two orders of magnitude.

The strong decrease of the hole current from the PEDOT: PSS contact with increasing content of inert matrix, combined with the much less affected hole current injected from the MoO_3 contact, indicates that there is a hindered injection of holes from the PEDOT: PSS into the MEH-PPV: NOA83H blend. A possible origin might be a vertical phase segregation in the blend such that there is an enriched NOA83H composition at the PEDOT: PSS interface. In a typical PLED the anode consists of ITO covered with a layer of PEDOT: PSS. Consequently, for application in a PLED a MEH-PPV: NOA83H blend with limited hole injection is not really suitable.

2.2.2. MEH-PPV: SR540 Blends

To verify whether this PEDOT: PSS contact problem is characteristic for NOA83H, the hole transport of blends using a different cross-linkable matrix, SR540, is investigated. To this end, hole only devices of MEH-PPV: SR540 blends with the same device structure were made and cross-linked with a dose of 43 J cm^{-2}. **Figure 3**a shows the *J*–*V* characteristics at room temperature of MEH-PPV: SR540 hole only devices from pristine (100:0) MEH-PPV down to 10:90 MEH-PPV: SR540. The curve of the pristine MEH-PPV (black squares) is again symmetric in forward- and reverse bias. In contrast to the mixtures based on NOA83H, here the current density of all blends is symmetric in forward- and reverse bias. In Figure 3b the current density at +2 (PEDOT: PSS) and −2 V (MoO_3), corrected for the film thickness, is plotted as a function of MEH-PPV concentration. From pristine MEH-PPV toward a 50:50 MEH-PPV: SR540 blend the current density gradually decreases one order of magnitude. For blends with a higher concentration of SR540 (25:75 and 10:90 MEH-PPV: SR540) the current density decrease is more pronounced. This shows that SR540 does not affect the hole injection in the blend and both contacts remain ohmic.

The absence of contact problems allows us to further investigate the hole transport of the MEH-PPV: SR540 blends. To this end, temperature-dependent *J*–*V* measurements were carried out. The *J*–*V* curves were fitted using drift-diffusion simulations[30] that include a temperature-, electric field-, and carrier

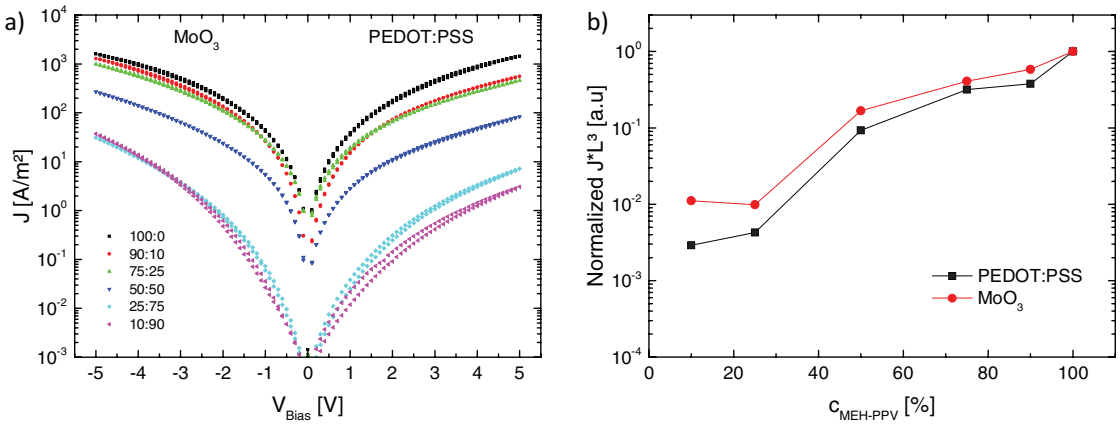

Figure 3. a) Current density–voltage characteristics at room temperature of MEH-PPV: SR540 hole only devices. Forward bias shows injection from PEDOT: PSS, reverse bias shows injection from MoO_3. b) Current density at +2 V (injection from PEDOT: PSS, black) and −2 V (injection from MoO_3, red) corrected for the film thickness. The blends were cross-linked with a dose of 43 J cm^{-2}.

density-dependent mobility.[31] The mobility is characterized by the following parameters; the mobility prefactor μ_0, the distance between transport sites a, and the width of the Gaussian density of states σ. The J–V characteristics for pristine MEH-PPV at different temperatures from 295 K down to 213 K are shown in **Figure 4**a. The J–V characteristics of 90:10, 75:25, and 50:50 MEH-PPV: SR540 blends can be found in Figure S3 (Supporting Information). The room temperature mobility at zero field for pristine MEH-PPV is 5×10^{-11} m^2 V^{-1} s^{-1}. The temperature dependence of the J–V characteristics is well described by the mobility parameters $\mu_0 = 11\,000$ m^2 V^{-1} s^{-1}, $a = 1.7$ nm, and $\sigma = 0.14$ eV. These values are in agreement with earlier reported values in literature.[31,32]

The J–V characteristics of the 90:10 to 50:50 MEH-PPV: SR540 blend hole-only devices have a similar voltage- and temperature dependence as that of the pristine MEH-PPV, except that the current is lower. As a result, the hole transport in the blends can be described with the same parameters $a = 1.7$ nm and $\sigma = 0.14$ eV as in pristine MEH-PPV. Only the mobility prefactor μ_0 had to be lowered to fit the reduced current density. The values of μ_0 versus the concentration of MEH-PPV in the blend are plotted in Figure 4b). With increasing amount of SR540 the mobility gradually decreases. In a blend with little amount of SR540, e.g., 90:10, the mobility is about half of the value for the pristine device. For the 50:50 MEH-PPV: SR540 blend the mobility decrease by a factor of 5 compared to pristine MEH-PPV. The identical temperature dependence of pristine MEH-PPV as compared to the MEH-PPV: SR540 blends, reflected by the unchanged σ, shows that the energetic disorder is not really affected by the addition of the SR540 matrix in this concentration regime.

2.3. Electron Transport in MEH-PPV: SR540 Blends

In MEH-PPV the electron and hole mobility are equal.[33] With the hole mobility known, we can further investigate the electron transport in the blends. Since addition of the matrix SR540 does not give rise to injection problems at the PEDOT: PSS contact, that might hinder the performance of blend-based PLEDs, we focus on MEH-PPV: SR540 blends.

Electron-only devices of MEH-PPV: SR540 blends were fabricated and the current density versus voltage was measured at different temperatures. The blends were cross-linked with

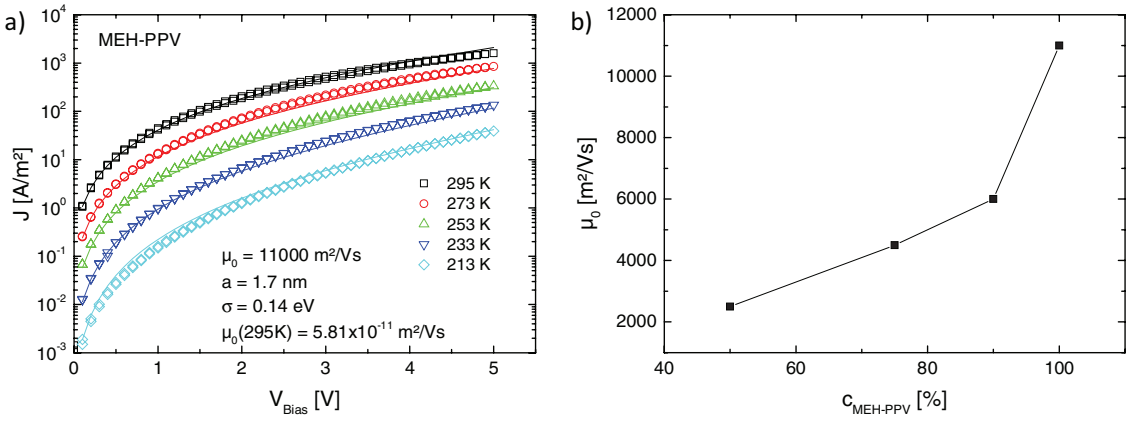

Figure 4. a) Current density–voltage characteristics of MEH-PPV for different temperatures (symbols) and drift-diffusion simulations using a temperature, field, and carrier density-dependent mobility (lines). b) Mobility prefactor μ_0 as a function of the MEH-PPV concentration in the blend with SR540.

a dose of 43 J cm^{-2}. The device structure of the electron only devices is Al/MEH-PPV: SR540/Ba/Al. The electron current in organic semiconductors is known to be trap limited.[34] The current density does not scale with $\frac{V^2}{L^3}$, like in the trap-free space-charge limited case,[32] but with $\frac{V^{r+1}}{L^{2r+1}}$.[35] The coefficient r relates to the width of the energy distribution of the traps and can be determined from the slope of the J–V characteristics on a double logarithmic axis. For MEH-PPV the coefficient r is typically equal to 4, leading to a thickness dependence scaling of L^9. To exclude the influence of a variation in film thickness on the J–V characteristics of the MEH-PPV: SR540 electron-only blend devices, the current density was multiplied by L^9 and normalized to the current density of pristine MEH-PPV at 6 V.

For the different blend concentrations ranging from pristine MEH-PPV (100:0) to 50:50 MEH-PPV: SR540, the thickness-corrected electron currents at room temperature are shown in **Figure 5**a. Remarkably, the electron current shows almost no dependence on the amount of SR540 in the blend. This is different to the hole transport, where the current density and mobility decreased with increasing amount of SR540 (Figure 3). Such a decrease of the hole and electron mobility is also expected to lead to a decrease of the trap-limited electron transport.

To further investigate the electron transport we performed temperature scans of the electron currents for the various blend composition. Figure 5b shows temperature-dependent J–V scans of a 90:10 MEH-PPV: SR540 blend-based electron only device. For modeling of the devices, the electron mobility is taken equal to the hole mobility.[33] To account for the trapping, traps with a Gaussian distribution in energy were used with the parameters trap density N_t, the trap depth E_t, and the width of the trap distribution σ_t.[34] A good agreement between simulation and measurement was obtained with $N_t = 1.0 \times 10^{23}$ m^{-3}, $E_t = 0.7$ eV, and $\sigma_t = 0.05$ eV, in agreement with earlier reported values.[36] The temperature scans and simulation of the 100:0, 80:20, and 50:50 MEH-PPV: SR540 can be found in Figure S4 (Supporting Information).

The obtained trap density as a function of the MEH-PPV fraction in the blend is shown in Figure 5c. We observe that with increasing amount of SR540, the trap density decreases. In the simulations the trap energy and width are kept constant at $E_t = 0.7$ eV and $\sigma_t = 0.05$ eV, respectively. The decrease of the trap density seems to correlate to the decrease in volume fraction of MEH-PPV in the blend, which is shown in red in Figure 5c.

The SR540 matrix is an insulator with a high band gap and is electrically inactive. This trap dilution effect has recently been observed for blends of MEH-PPV and a number of large band gap polymers as polystyrene, polyvinylcarbazole, and polyfluorene.[37] A condition for trap dilution to occur is that there is no macroscopic phase separation. To check, if phase separation occurs an AFM topography picture of a 50:50 MEH-PPV: SR540 blend was measured (see Figure S5, Supporting Information). We observe that the surface is smooth and featureless and does not indicate any form of phase separation.[38] The same was observed for other blend compositions. So the fact that the trap-limited electron current seems nearly independent on the fraction of insulating SR540 in the blend is a result of two effects that counteract; the decrease of the charge carrier mobility is compensated by the dilution of the trapping sites.

In summary, the hole and electron transport in the 90:10 MEH-PPV: SR540 blend is nearly identical to the transport in pristine MEH-PPV. This demonstrates that MEH-PPV is not damaged by the exposure to UV-light. MEH-PPV is known to photo-oxidize if illuminated with UV-light in the presence of oxygen.[39] In this case the electron transport would be strongly decreased because photo-oxidation generates carbonyl groups that act as electron traps. To check if the carbonyl groups are formed during UV-illumination Fourier transform infrared spectroscopy was done. A reference sample of MEH-PPV was not illuminated with UV light and compared to a MEH-PPV sample that was illuminated with a dose of 40 J cm^{-2}. The spectra can be found in Figure S6 (Supporting Information). In the case of photo-oxidation, carbonyl groups that show a strong absorption around 1650 cm^{-1} are formed.[39] Neither the pristine MEH-PPV nor the UV-illuminated MEH-PPV samples show a strong peak in this region, proving that MEH-PPV is not damaged during the UV-illumination in nitrogen.

2.4. 90:10 MEH-PPV: SR540 PLED

In order to make MEH-PPV insoluble to chlorobenzene we have observed that only 10% of the UV-curable SR540 matrix is necessary to make the blend insoluble. These 10% of SR540

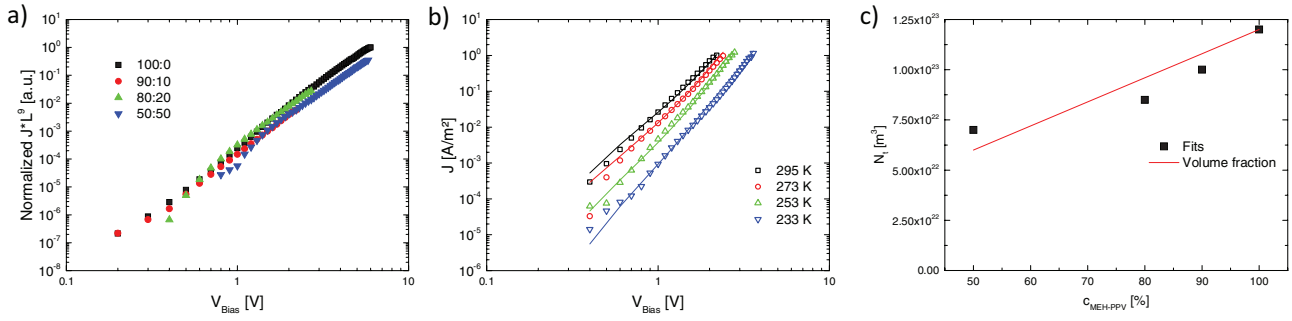

Figure 5. a) Current density–voltage characteristics at room temperature of MEH-PPV: SR540 electron-only devices after correction for the film thickness. b) Temperature-dependent current density–voltage characteristics of 90:10 MEH-PPV: SR540 electron-only devices. The solid lines show fits with $N_t = 1.0 \times 10^{23}$ m^{-3}, $E_t = 0.7$ eV, and $\sigma_t = 0.05$ eV. c) Trap density versus the MEH-PPV concentration from the simulations (black) compared to the decrease of volume fraction of MEH-PPV (red). The blends were cross-linked with a dose of 43 J cm^{-2}.

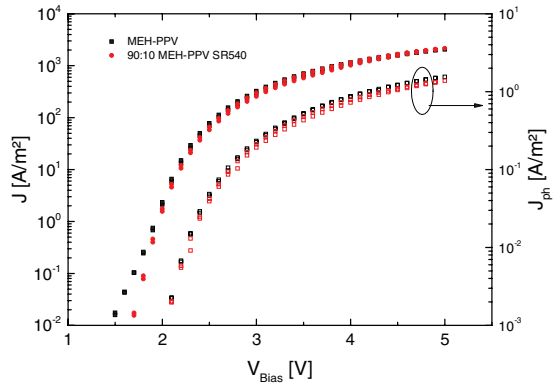

Figure 6. Current density (J) and photocurrent (J_{ph}) plotted as a function of voltage (V) for PLED devices based on pristine MEH-PPV (black) and the 90:10 MEH-PPV: SR540 blend (red).

only slightly reduce the charge carrier mobility, resulting in decreased hole current density. On the other hand, the trap density is diluted, giving an increase of the electron current density. To observe how both effects influence the current density in a PLED double carrier devices were made using a 90:10 MEH-PPV: SR540 blend that is cross-linked with a dose of 43 J cm^{-2}. As a reference, also a PLED of pristine MEH-PPV is simultaneously fabricated. The device structure of the blend PLEDs is ITO/PEDOT: PSS/MEH-PPV: SR450/Ba/Al. Current density as well as the photocurrent density is shown in **Figure 6** for both blend and pristine device. The current and photocurrent are equal for both devices. The electroluminescence spectra of both devices are shown in Figure S7 (Supporting Information). No significant differences are observed, expect for a slightly enhanced emission corresponding to the 0–1 transition. However, this is likely due to a difference in optical thickness between the films. The efficiency, the photocurrent divided by the electric current, is also identical. This also confirms that the MEH-PPV is not damaged by the UV treatment. As a result, it is demonstrated that the processability of a standard conjugated polymer as MEH-PPV can be modified without affecting its functional properties. This result enables us to stack these insoluble MEH-PPV-based blend films in a solution-processed multilayer device.[40]

3. Summary

In conclusion, a generic method to tune the solubility of a MEH-PPV layer by blending it with a UV-curable matrix is demonstrated. For two different matrices, NOA83H and SR540, only 10% of matrix is needed to get an insoluble layer. However, the NOA83H matrix affects the hole injection from the PEDOT: PSS contact, which is not observed when SR540 is used. The hole mobility of 90:10 MEH-PPV: SR540 blends is only slightly lower as compared to pristine MEH-PPV. For the electron transport the mobility decrease is compensated by a dilution of the trap concentration. As a result PLEDs based on an insoluble 90:10 MEH-PPV: SR540 blend exhibit identical current density and photocurrent as compared to pristine MEH-PPV.

4. Experimental Section

The chemical structure of the materials used in this work is shown in Figure S1 (Supporting Information). The structure of NOA83H is not known.

Water-free chlorobenzene was used as solvent for all materials. For MEH-PPV a concentrations of 5.5 mg mL^{-1} was typically used, whereas for the matrices NOA83H and SR540 20 and 40 mg mL^{-1} were used, respectively. In order to activate the cross-linking process of SR540, the photoinitiator Irgacure 819 (BASF SE) was added with a concentration of 2 wt% relative to the total material in the blend solution. PLEDs as well as hole-only devices were processed on a glass substrate with a prepatterned indium tin oxide (ITO) layer. The substrates were cleaned using soap followed by an ultrasonic acetone and isopropanol bath. After that they were dried and treated with UV-ozone. PEDOT: PSS (Clevios P VP Al 4083, Heraeus) was spin coated with a speed of 250 rpm for 10 s followed by a drying step with 1500 rpm for 50 s. The layer was baked at 140 °C for 10 min, resulting in 45 nm thick films. The MEH-PPV: matrix blends were spin coated in a nitrogen atmosphere with a speed of 1000 rpm for 20 s, followed by 250 rpm for 90 s. For pristine MEH-PPV or for blends with a matrix content <10%, this procedure typically gives dry films with an average thickness of ≈100 nm. The blend was then cross-linked in a nitrogen atmosphere with a Dymax 2000-EC UV flood lamp. The spectral output and the absorption spectrum of MEH-PPV are shown in Figure S2 (Supporting Information). The photoinitiator Irgacure 819 is sensitive to wavelengths below 400 nm. Cathodes were thermally evaporated at a pressure of 10^{-6} mbar. For electron-only and PLEDs cathodes consisted of 5 nm barium and 100 nm aluminum as a capping layer. For electron-only devices the anode consisted of a 30 nm aluminum layer that was slightly oxidized. For hole-only devices the top electrode was made of 10 nm MoO_3 followed by a 100 nm Al capping layer. The devices were characterized in nitrogen atmosphere using a Keithley 2400 source meter and a 6514 system electrometer connected to a Si-photodiode. The film thickness was measured with a Bruker DektakXT Stylus Profiler. The topography was analyzed using a Nanoscope Dimension 3100 (Bruker) atomic force microscope.

Supporting Information

Supporting Information is available from the Wiley Online Library or from the author.

Acknowledgements

This work was supported by the Dutch Polymer Institute (DPI), Project No. 748.

Keywords

charge transport, polymer light-emitting diodes, solution processing

Received: November 25, 2016
Revised: January 25, 2017
Published online: April 7, 2017

[1] B. W. D'Andrade, M. A. Baldo, C. Adachi, J. Brooks, M. E. Thompson, S. R. Forrest, *Appl. Phys. Lett.* **2001**, *79*, 1045.
[2] W. L. Ma, P. K. Iyer, X. Gong, B. Liu, D. Moses, G. C. Bazan, A. J. Heeger, *Adv. Mater.* **2005**, *17*, 274.
[3] T. L. Ye, M. R. Zhu, J. S. Chen, D. G. Ma, C. L. Yang, W. F. Xie, S. Y. Liu, *Org. Electron.* **2011**, *12*, 154.

[4] K. S. Yook, S. E. Jang, S. O. Jeon, J. Y. Lee, *Adv. Mater.* **2010**, *22*, 4479.
[5] S. Sax, N. Rugen-Penkalla, A. Neuhold, S. Schuh, E. Zojer, E. J. W. List, K. Mullen, *Adv. Mater.* **2010**, *22*, 2087.
[6] C. M. Zhong, C. H. Duan, F. Huang, H. B. Wu, Y. Cao, *Chem. Mater.* **2011**, *23*, 326.
[7] C. Tanase, J. Wildeman, P. W. M. Blom, *Adv. Funct. Mater.* **2005**, *15*, 2011.
[8] R. Trattnig, L. Pevzner, M. Jäger, R. Schlesinger, M. V. Nardi, G. Ligorio, C. Christodoulou, N. Koch, M. Baumgarten, K. Müllen, E. J. W. List, *Adv. Funct. Mater.* **2013**, *23*, 4897.
[9] S. Xue, X. Qiu, L. Yao, L. Wang, M. Yao, C. Gu, Y. Wang, Z. Xie, H. Wu, *Org. Electron.* **2015**, *27*, 35.
[10] N. Aizawa, Y.-J. Pu, M. Watanabe, T. Chiba, K. Ideta, N. Toyota, M. Igarashi, Y. Suzuri, H. Sasabe, J. Kido, *Nat. Commun.* **2014**, *5*, 5756.
[11] L. Derue, S. Olivier, D. Tondelier, T. Maindron, B. Geffroy, E. Ishow, *ACS Appl. Mater. Inter.* **2016**, *8*, 16207.
[12] M. C. Gather, A. Kohnen, A. Falcou, H. Becker, K. Meerholz, *Adv. Funct. Mater.* **2007**, *17*, 191.
[13] C. Gu, T. Fei, L. A. Yao, Y. Lv, D. Lu, Y. G. Ma, *Adv. Mater.* **2011**, *23*, 527.
[14] A. Haldi, A. Kimyonok, B. Domercq, L. E. Hayden, S. C. Jones, S. R. Marder, M. Weck, B. Kippelen, *Adv. Funct. Mater.* **2008**, *18*, 3056.
[15] A. Kohnen, N. Riegel, J. H. W. M. Kremer, H. Lademann, D. C. Muller, K. Meerholz, *Adv. Mater.* **2009**, *21*, 879.
[16] J.-S. Kim, R. H. Friend, I. Grizzi, J. H. Burroughes, *Appl. Phys. Lett.* **2005**, *87*, 023506.
[17] X. H. Yang, F. Jaiser, B. Stiller, D. Neher, F. Galbrecht, U. Scherf, *Adv. Funct. Mater.* **2006**, *16*, 2156.
[18] L. Duan, B. D. Chin, N. C. Yang, M.-H. Kim, H. D. Kim, S. T. Lee, H. K. Chung, *Synth. Met.* **2007**, *157*, 343.
[19] R.-Q. Png, P.-J. Chia, J.-C. Tang, B. Liu, S. Sivaramakrishnan, M. Zhou, S.-H. Khong, H. S. O. Chan, J. H. Burroughes, L.-L. Chua, R. H. Friend, P. K. H. Ho, *Nat. Mater.* **2010**, *9*, 152.
[20] S.-R. Tseng, H.-F. Meng, C.-H. Yeh, H.-C. Lai, S.-F. Horng, H.-H. Liao, C.-S. Hsu, L.-C. Lin, *Synth. Met.* **2008**, *158*, 130.
[21] S.-R. Tseng, S.-C. Lin, H.-F. Meng, H.-H. Liao, C.-H. Yeh, H.-C. Lai, S.-F. Horng, C.-S. Hsu, *Appl. Phys. Lett.* **2006**, *88*, 163501.
[22] H. A. Al-Attar, A. P. Monkman,*J. Appl. Phys.* **2011**, *109*, 074516.
[23] K. D. He, Y. Liu, J. Y. Gong, P. Zeng, X. Kong, X. L. Yang, C. Yang, Y. Yu, R. Q. Liang, Q. R. Ou, *Appl. Surf. Sci.* **2016**, *382*, 288.
[24] S. Ho, S. Liu, Y. Chen, F. So, *J. Photonics Energy.* **2015**, *5*, 057611.
[25] Z.-L. Zhou, X. Sheng, K. Nakua, L. Zhao, G. Gibson, S. Lam, C. C. Yang, J. Brug, R. Elder, *Appl. Phys. Lett.* **2010**, *96*, 013504.
[26] No thickness decrease upon curing was observed.
[27] This experiment has been performed with an MEH-PPV concentration slightly lower than the typical value of 5.5 mentioned in the Experimental Section, hence the somewhat reduced initial film thickness.
[28] G. A. H. Wetzelaer, P. W. M. Blom, *Phys. Rev. B* **2014**, *89*, 241201.
[29] N. F. Mott, R. W. Gurney, *Electronic Processes in Ionic Crystals*, Oxford University Press, London **1940**.
[30] L. J. A. Koster, E. C. P. Smits, V. D. Mihailetchi, P. W. M. Blom, *Phys. Rev. B* **2005**, *72*, 085205.
[31] W. F. Pasveer, J. Cottaar, C. Tanase, R. Coehoorn, P. A. Bobbert, P. W. M. Blom, D. M. de Leeuw, M. A. J. Michels, *Phys. Rev. Lett.* **2005**, *94*, 206601.
[32] P. W. M. Blom, M. J. M. de Jong, J. J. M. Vleggaar, *Appl. Phys. Lett.* **1996**, *68*, 3308.
[33] Y. Zhang, B. de Boer, P. W. M. Blom, *Phys. Rev. B* **2010**, *81*, 085201.
[34] H. T. Nicolai, M. M. Mandoc, P. W. M. Blom, *Phys. Rev. B* **2011**, *83*, 195204.
[35] P. Mark, W. Helfrich, *J. Appl. Phys.* **1962**, *33*, 205.
[36] H. T. Nicolai, M. Kuik, G. A. H. Wetzelaer, B. de Boer, C. Campbell, C. Risko, J. L. Bredas, P. W. M. Blom, *Nat. Mater.* **2012**, *11*, 882.
[37] D. Abbaszadeh, A. Kunz, G. A. H. Wetzelaer, J. J. Michels, N. I. Craciun, K. Koynov, I. Lieberwirth, P. W. M. Blom, *Nat. Mater.* **2016**, *15*, 628.
[38] We note that the semi-fluid nature of the uncured film did not allow for microscopically characterizing the blend layer before curing.
[39] J. C. Scott, J. H. Kaufman, P. J. Brock, R. DiPietro, J. Salem, J. A. Goitia, *J. Appl. Phys.* **1996**, *79*, 2745.
[40] C. Kasparek, P. W. M. Blom, *Appl. Phys. Lett.* **2017**, *110*, 023302.

